International Journal of Bridge Engineering (IJBE), Vol. 10, No. 3, (2022), pp. 01-36

EFFICIENCY OF DYNAMIC RELAXATION METHODS IN SOLVING BENDING PLATES

Hossien Estiri[1] and Amir Baghban[2]

[1,2] Civil Engineering Dept., Gonabad University, Gonabad, Islamic Republic of Iran
e-mail: h.estiri@gonabad.ac.ir, abaghban@gonabad.ac.ir

ABSTRACT: The bending plate structure has been solved by several researchers with explicit dynamic relaxation (DR) methods. These techniques are based on the different assumptions. The main purpose of this paper is investigation the merit of various procedures for elastic analysis of bending plates. Therefore, sixteen known algorithms are employed. It should be reminded that the difference between these tactics is how to find the fictitious parameters of DR. Several examples of bending plates, with various shapes, are analyzed. According to number of iteration and duration analysis, the studied approaches of DR are graded. Finally, the ranking of these methods is found. The numerical results indicate the appropriate efficiency of Underwood and nodal damping processes for linear analysis of bending plates.

KEYWORDS: Dynamic relaxation; Mass; Damping; Time step; Bending plate.

1 INTRODUCTION

There are too many exact and numerical solutions to analyze the bending plates [1]. For the first time, the thin plates mathematical relations formulated by Euler. It should be added that the first governing differential equations of these structures obtained by Germain [2]. Kirchhoff proposed the complete theory of bending plates. He derived the plate differential equation based on Bernoulli's assumptions for beams [2]. Up to now, dynamic relaxation numerical solutions were used to analyze the various structures. Among the 60^{th} century, this approximate method used by Otter and Day [3-5]. Note that the DR approach is based on the Second-Order Richardson technique which was developed by Frankel [6]. The DR procedure use the different hypotheses. In other words, the fictitious parameters are achieved by these assumptions and the governing equations are converted from static form to dynamic. Moreover, the previous researches will be presented which have been performed in recent decade about DR fictitious parameters.

By using the first three terms of the Taylor series, displacement obtained by Rezaiee-Pajand and Taghavian Hakkak [7]. The fictitious time step was formulated by Kadkhodayan et al. based on minimizing the unbalanced forces

[8]. Rezaiee-Pajand and Alamatian performed the nonlinear dynamic analysis with DR tactic [9]. Another relation for optimal time step and critical damping was obtained by Rezaiee-Pajand and Sarafrazi [10]. Rezaiee-Pajand and Alamatian presented new formulas for the fictitious mass and damping [11]. In addition, Rezaiee-Pajand et al. established a new algorithm to evaluate the fictitious damping. They was used error minimization between two sequential steps [12]. Rezaiee-Pajand and Sarafrazi proposed another relation for the time step ratio by using zero damping [13]. Based on the residual energy, a new method suggested by Rezaiee-Pajand et al. to find the fictitious time step [14]. Alamatian was obtained a new fictitious mass formulation for the kinetic DR [15]. Rezaiee-Pajand et al. investigated the efficiency of twelve DR processes for finite element analysis of frames and trusses [16]. In addition, a new time step was presented by Rezaiee-Pajand and Rezaiee for the kinetic DR [17].

The ability of DR procedures in the bending plate analysis [18], three-dimensional frames with and without shear effects [19], as well as, shell [20] was evaluated by Rezaiee-Pajand and Estiri. It should be noted that these structures had geometric nonlinear behavior. In a comprehensive comparison study, the abilities of 51 different dynamic relaxation procedures were found, and the obtained results were presented [21]. Lee et al. used two implicit and explicit arc length processes to analyze the post-buckling of space frames [22]. Rezaiee-Pajand and Estiri also established four formulas to estimate the load factor for finding the structural static path [23-26]. Specifications of a lot of the DR schemes are discussed in two state of the art papers [27, 28].

Here, the application of the dynamic relaxation method in the analysis of bridges is expressed. Shoukry et al. used this technique in analyzing large transportation structures as dowel jointed concrete pavements and 306-m-long, reinforced concrete bridge superstructure under the effect of temperature variations [29]. Bagrianski and Halpern presented an adaptation of the DR method for the form-finding of small-strain. They used a new iterative technique termed Prescriptive Dynamic Relaxation (PDR). Case studies are a segmental concrete shell and a pedestrian steel bridge [30]. The DR method extended to accommodate friction effects in tensioned structures that include continuous cables [31]. The DR technique applied to analyze the responses of reinforced concrete bridge piers subjected to vehicle collision [32].

The nonlinear thermo-elastic bending analysis of a functionally graded carbon nanotube-reinforced composite plate resting on two parameter elastic foundations was investigated by Golmakani and Zeighami [33]. In another study, Golmakani and Kadkhodayan investigated the axisymmetric bending and stretching of circular and annular functionally graded plates with variable thickness under combined thermal-mechanical loading and various boundary conditions [34]. Four systematic approaches developed in the context of the indirect methods for analyzing the nonlinear prebuckling behavior [35]. The adaptive dynamic relaxation approach is used to solve linear elastic and crack

propagation problems [36].

As it was said; different methods have been proposed to determine the artificial parameters of the DR. However, the efficiency of these approaches in elastic analysis of bending plates has not been investigated. In this study, sixteen various and well-known procedures of the DR are used for linear analysis of the bending plates. The differences between these tactics cause from various artificial parameters of the DR solutions. In addition, the Dunkerley technique will be used by authors to evaluate the minimum frequency of dynamic system. It is mentioned that this algorithm has not been applied to determine the fictitious damping since now. On the other hand, the authors will be proposed fictitious parameters of several processes with another tactic calculates. After analyzing different structures and based on the number of iterations and duration of analysis, the DR approaches are ranked. Ultimately, the final ranking of each procedure was obtained.

2 THE DYNAMIC RELAXATION METHOD

In the DR process, an artificial dynamic system is provided by adding fictitious damping and mass matrices to the structural static equilibrium equations. The repeated relations of this solution which are obtained by using central finite differences tactics are defined as follow:

$$\dot{X}_i^{n+\frac{1}{2}} = \frac{2m_{ii}^n - C_{ii}^n t^n}{2m_{ii}^n + C_{ii}^n t^n} \dot{X}_i^{n-\frac{1}{2}} + \frac{2t^n}{2m_{ii}^n + C_{ii}^n t^n}(p_i^n - f_i^n) \quad , \quad i = 1,2,\ldots,ndof \tag{1}$$

$$X_i^{n+1} = X_i^n + t^{n+1} \dot{X}_i^{n+\frac{1}{2}} \quad , \quad i = 1,2,\ldots,ndof \tag{2}$$

The i^{th} diagonal element of fictitious damping and mass matrices, time step and i^{th} element of internal force vector at the n^{th} iteration of the DR are assigned with m_{ii}^n t^n ، C_{ii}^n ،and f_i^n , respectively. The external force of static system is p_i^n . Moreover, *ndof* shows the number of degrees of freedom for system. Furthermore, the vectors X and $\dot{X}$ indicate the displacement and velocity, correspondingly. It is mentioned that the relations of DR are explicit and only performed by vector calculations. The residual force R can be obtained in the below form:

$$\mathbf{R} = \mathbf{P} - \mathbf{F} \tag{3}$$

Now, the well-known techniques of DR for calculating the fictitious parameters will be defined.

2.1 Papadrakakis method

Eq. (4) proposed by Papadrakakis to find the mass and damping matrices [37]. Here, the fictitious factors of mass and damping are denoted by ρ and c, respectively. Also, the matrix D is diagonal. The elements of matrix D are the

same as the diagonal entries of the stiffness matrix. Eqs. (5) and (6) are used to calculate the optimal factors:

$$\mathbf{M} = \rho\mathbf{D} \quad , \quad \mathbf{C} = c\mathbf{D} \tag{4}$$

$$\left(\frac{t^2}{\rho}\right)_{opt} = \frac{4}{\lambda_{B\,max} + \lambda_{B\,min}} \tag{5}$$

$$\left(\frac{ct}{\rho}\right)_{opt} = \frac{4\sqrt{\lambda_{B\,max}.\lambda_{B\,min}}}{\lambda_{B\,max} + \lambda_{B\,min}} \tag{6}$$

The symbols $\lambda_{B\,min}$ and $\lambda_{B\,max}$ are the minimum and maximum eigenvalues of matrix B ($\mathbf{B} = \mathbf{D^{-1}S}$). These values can be calculated with Eqs. (7) and (8). The rate of error reduction between two successive iteration is showed with λ_{DR} which is evaluated by Eq. (9). First, the values of $\lambda_{B\,min}$ and $\lambda_{B\,max}$ are assumed and the DR process begins. When the quantity of λ_{DR} is converged to a constant value, $\lambda_{B\,min}$ is achieved by Eq. (7). In Papadrakakis algorithm, time step is constant and equal to one.

$$\lambda_{B\,min} = -\frac{\lambda_{DR}^2 - \frac{4}{2+ct/\rho}\lambda_{DR} + \frac{2-ct/\rho}{2+ct/\rho}}{\frac{2t^2/\rho}{2+ct/\rho}\lambda_{DR}} \tag{7}$$

$$\left|\lambda_{B\,max}\right| < \max_i \sum_{j=1}^{ndof} \left|b_{ij}\right| \tag{8}$$

$$\lambda_{DR} = \frac{\left\| X^{n+1} - X^{n} \right\|}{\left\| X^{n} - X^{n-1} \right\|} \tag{9}$$

2.2 Underwood procedure

Underwood obtained the mass matrix with Eq. (10). In this relation, the value of time step is equal to 1.1. Moreover, the minimum frequency of artificial dynamic system ω_0 is evaluated in Eq. (11). This equation shows the Rayleigh principle. It should be added that the relation of fictitious damping is $\mathbf{C} = \mathbf{2\omega_0 M}$.

$$m_{ii} = \frac{t^2}{4} \sum_{j=1}^{ndof} \left|S_{ij}\right| \tag{10}$$

$$\omega_0 = \sqrt{\frac{\mathbf{X^T S^L X}}{\mathbf{X^T M X}}} \tag{11}$$

Where S^L is the local stiffness matrix and its entries are determined with Eq. (12) [38]. It is mentioned that if the index expression of the square root in Eq.

(11) was negative, the damping is assumed to be equal to zero. Furthermore, if ω_0 was greater than 2, a value lower than 2 (e.g. 1.9) is used in calculations.

$$S_{ii}^{L,n} = \frac{f_i(X^n) - f_i(X^{n-1})}{\dot{t}^{\,n-\frac{1}{2}} \dot{X}_i} \tag{12}$$

2.3 Qiang tactic

In this method, the mass matrix is evaluated by Eq. (13). This relation shows the superposition of absolute values of row elements of stiffness matrix. In addition, to determine the damping and time step, Eqs. (14) and (15) were proposed by Qiang [39].

$$m_{ii} = \sum_{j=1}^{ndof} \left| S_{ij} \right| \tag{13}$$

$$C_{ii} = 2\sqrt{\frac{\omega_0}{1+\omega_0}} m_{ii} \tag{14}$$

$$t = \frac{2}{\sqrt{1+\omega_0}} \tag{15}$$

Also, the minimum frequency of system in the free vibration is obtained by using Rayleigh principle as below [39]. Here, the stiffness matrix has been assigned by S.

$$\boldsymbol{\omega_0} = \frac{\mathbf{X^T S X}}{\mathbf{X^T M X}} \tag{16}$$

2.4 Zhang approach

Zhang and Yu assumed that the relation of damping is as follow [40]:

$$\boldsymbol{\omega_0} = \frac{\mathbf{X^T F}}{\mathbf{X^T M X}} \tag{17}$$

$$\mathbf{C} = \mathbf{2\omega_0 M} \tag{18}$$

The fictitious mass matrix is achieved in Eq. (10) with the time step of one. It should be added that they proposed non-zero initial displacements instead of using zero vector. Rezaiee-Pajand et al. indicated that calculating the initial displacement according to Zhang's scheme has not enough efficiency [16]. Thus, in this paper, the zero vector is used to start the DR process.

2.5 The nodal damping algorithm

Kadkhodayan et al. suggested that the nodal damping applied instead of the same damping factor in all degrees of freedom. In other words, the damping

parameter is similar for all DOFs of one node. They obtained the following relation to calculate the damping factor [41].

$$C_k = \zeta_k m_{kk} \qquad k = 1,2,...,N \tag{19}$$

$$\zeta_k^n = 2\left[\frac{(X_k^n)^T f_k^n}{(X_k^n)^T m_{kk}^n (X_k^n)}\right]^{\frac{1}{2}} \tag{20}$$

The number of structure nodes is shown with N. The fictitious mass matrix is evaluated in Eq. (10) with the time step of one.

2.6 Rezaiee-Pajand and Taghavian Hakkak technique

Rezaiee-Pajand and Taghavian Hakkak assumed that the diagonal entries of mass matrix are proportional with the corresponded values of these in stiffness matrix. The Eq. (21) shows the mathematical approach of this procedure [7]. These researchers proposed $\alpha = 0.6$.

$$m_{ii} = \alpha . S_{ii} \tag{21}$$

In this tactic, the damping is obtained from Qiang method. Also, the time step is equal to one. It should be added that displacement is calculated by Eq. (22) instead of Eq. (2). The acceleration $\ddot{X}^n$ and velocity $\dot{X}^n$ can be evaluated by Eqs. (23) and (24) [7].

$$X^{n+1} = X^n + t\dot{X}^n + \frac{t^2}{2}\ddot{X}^n \tag{22}$$

$$R^n = M^n \ddot{X}^n + C^n \dot{X}^n \tag{23}$$

$$\dot{X}^n = \frac{X^n - X^{n-1}}{t} \tag{24}$$

2.7 Kinetic damping process

In the kinetic DR method, the damping C is equal to zero. When the kinetic energy is reduced, a peak point in the kinetic energy graph is passed. At this time and to restart the DR process, the displacements and velocities are obtained with Eqs. (25) and (26), respectively. In Eq. (26), the residual force vector r_i^n is calculated at the position $X_i^{n-\frac{1}{2}}$, obtained in Eq. (25) [42].

$$X_i^{n-\frac{1}{2}} = X_i^{n+1} - \frac{3}{2}t\dot{X}_i^{n+\frac{1}{2}} + \frac{t^2}{2m_{ii}}r_i^n \tag{25}$$

$$\dot{X}_i^{n+\frac{1}{2}} = \frac{t}{2m_{ii}} r_i^n \tag{26}$$

Then, the iterations of DR begin by these vectors of displacement and velocity until the kinetic energy is maximum again. This process continues to achieve the response. The fictitious time step in this algorithm is equal to one. Furthermore, the mass matrix is obtained with Eq. (27) [43].

$$m_{ii} = \frac{t^2}{2} \sum_{j=1}^{ndof} \left| S_{ij} \right| \tag{27}$$

2.8 Minimum residual force method

Kadkhodayan et al. was written the unbalanced force function of the artificial dynamic system by utilizing Eq. (28). By minimizing this function with respect to time step, the Eq. (29) is obtained [8]. In this relation, $\dot{f}_i^{n+\frac{1}{2}}$ is the internal force increment. This value can be evaluated in Eq. (30) [14]:

$$UBF = \sum_{i=1}^{ndof} \left[r_i^n - t^{n+1} \dot{f}_i^{n+\frac{1}{2}} \right]^2 \tag{28}$$

$$t^{n+1} = \frac{\sum_{i=1}^{ndof} r_i^n \dot{f}_i^{n+\frac{1}{2}}}{\sum_{i=1}^{ndof} \left(\dot{f}_i^{n+\frac{1}{2}} \right)^2} \tag{29}$$

$$\dot{f}_i^{n+\frac{1}{2}} = \sum_{j=1}^{ndof} S_{ij,T}^n \dot{X}_i^{n+\frac{1}{2}} \tag{30}$$

Here, the tangent stiffness matrix is $S_{ij,T}^n$. In addition, the fictitious mass and damping matrices are calculated with Eqs. (10) and (18), respectively.

2.9 Rezaiee-Pajand and Alamatian procedure

Another relation was obtained by Rezaiee-Pajand and Alamatian for fictitious mass [11]. In addition, the calculation of damping is done with Eq. (32) [11]. It is mentioned that the minimum of artificial frequency ω_0 is evaluated in Eq. (17). Moreover, the time step is constant and equal to one.

$$m_{ii} = Max\left(\frac{(t^n)^2}{2} S_{ii}^n, \frac{(t^n)^2}{2} \sum_{j=1}^{ndof} \left|S_{ij}^n\right|\right) \tag{31}$$

$$C_{ii} = \sqrt{\omega_0^2 (4 - t^2 \omega_0^2)} m_{ii} \tag{32}$$

2.10 Minimum unbalanced energy tactic

The out-of-balance energy function is obtained as follow [14]:

$$UBE = \sum_{i=1}^{ndof} \left[t^{n+1} \dot{X}_i^{n+\frac{1}{2}} \left(r_i^n - t^{n+1} \dot{f}_i^{n+\frac{1}{2}} \right) \right]^2 \tag{33}$$

Rezaiee-Pajand et al. minimized the Eq. (33). This operation is caused to obtain two values for the time step. One of these is minimized the unbalanced energy function. On the other hand, if the characteristic equation (33) has no real answer, the Eq. (29) is used to evaluate the time step. Note that the mass and damping matrices are achieved in Eqs. (31) and (32), correspondingly.

2.11 Rezaiee-Pajand and Sarafrazi approach

A method based on the power iteration process was proposed by Rezaiee-Pajand and Sarafrazi to evaluate the damping matrix [10]. They used a step of power iteration algorithm in each iteration of DR. The damping matrix is obtained as below:

$$C_{ii}^n = \sqrt{\lambda_1^n (4 - \lambda_1^n)} m_{ii}^n \tag{34}$$

Here, $\lambda_1^n = \lambda^n + 4$ and it is known as transferred eigenvalue. The factor λ^n is the eigenvalue in the power iteration solution. In each step of DR, this factor is compared with the eigenvalue obtained in Rayleigh principle and the lower value is selected. Furthermore, the time step is one and the mass is evaluated by Eq. (31).

2.12 Zero damping technique

By using of zero damping, Rezaiee-Pajand and Sarafrazi proposed the Eq. (35) for the time step ratio γ [13]. Also, the method of power iteration is used to evaluate the minimum eigenvalue λ_1. In this procedure, the mass matrix is obtained in Eq. (31). Moreover, the determination of displacement and velocity vectors is performed in Eqs. (36) and (37) [13]. Thus, Eqs. (1) and (2) do not require in this tactic.

$$\gamma = \frac{t^{n+1}}{t^n} = \frac{1}{\left(1 + \sqrt{\lambda_1}\right)^2} \tag{35}$$

$$\dot{\mathbf{X}}^{\mathbf{n+1}} = \boldsymbol{\gamma}^{\mathbf{n}} \left(\mathbf{M}^{-1}\mathbf{R} + \dot{\mathbf{X}}^{\mathbf{n}} \right) \tag{36}$$

$$\mathbf{X}^{\mathbf{n+1}} = \mathbf{X}^{\mathbf{n}} + \dot{\mathbf{X}}^{\mathbf{n+1}} \tag{37}$$

2.13 Dunkerley algorithm

In this method, the frequency is obtained in Eq. (38). Here, the term $a_{ii}m_{ii}$ shows the contribution of each degree of freedom in the absence of others. Thus, the relation of Dunkerley is changed to Eq. (39) [44]:

$$\frac{1}{\omega_0^2} = \sum_{i=1}^{ndof} a_{ii}m_{ii} \tag{38}$$

$$\frac{1}{\omega_0^2} = \sum_{i=1}^{ndof} \frac{1}{\omega_{ii}^2} \tag{39}$$

Where ω_{ii}^2 is the frequency of SDOF system with mass m_{ii} in ith degree of freedom. The mass and damping matrices are evaluated with Eqs. (31) and (32), respectively. Also, the time step one is used. It is mentioned, the Dunkerley process provides a lower bound for main frequency of vibration [44].

3 NUMERICAL EXAMPLES

In this section, different plates will be linearly analyzed with the methods defined in previous section. The results of several benchmarks are obtained by applying the entire loads in ten steps. Then, some new problems will be solved. The number of iterations and the analysis durations in each sample are found. It is mentioned that these methods have a same accuracy. However, the number of iterations to achieve the response is various. The dynamic relaxation process to analyze the structures is performed as below:

- Step 1- The initial values of velocity is assumed to be zero. Also, the initial displacement is equal to zero vector or convergence displacement of the previous increment.
- Step 2- The vector of internal forces and the stiffness matrix are provided for each element of structure. By superposition of all internal force vectors, the vector of global internal forces of structure is obtained.
- Step 3- The residual force vector is evaluated from Eq. (3).
- Step 4- If $\sqrt{\sum_{i=1}^{ndof} \left(r_i^n\right)^2} \le e_R$, go to Step 9; otherwise, continue.
- Step 5- Construct the fictitious mass and damping matrices.
- Step 6- The velocities are updated with Eq. (1).

- Step 7- The time step is adapted.
- Step 8- The nodal displacements are updated with Eq. (2) and the analysis is followed from Step 2.
- Step 9- Print the displacements.
- Step 10- If $N > 10$, the process is finish; otherwise $N = N + 1$ and then, it is continued from Step 2.

The number of increments is defined with N. It should be added that the acceptable residue force error is assumed to be 10^{-4} for all methods. The thickness of plates (h), module of elasticity (E) and Poisson ratio (υ) are equal to 1 cm, 200 GPa and 0.3, respectively. In addition, the maximum deflection has been occurred in point M. The following relations evaluate the degree of merit for studied procedures:

$$E_I = 100 \times \left(\frac{I_{max} - I}{I_{max} - I_{min}} \right) \tag{40}$$

$$E_T = 100 \times \left(\frac{T_{max} - T}{T_{max} - T_{min}} \right) \tag{41}$$

The number of iterations, duration of analysis, score based on the number of iteration and score based on the duration of analysis are shown by I, T, E_I and E_T, correspondingly. The approach with the highest number of iteration and duration of analysis has score zero. Also, the score of 100 is assigned to the tactic with lowest number of iteration and duration of analysis. The score of each technique supplies the rank of that. For better comparison, the authors have suggested the fictitious parameters of some processes obtained by other method. Table 1 show the different algorithms used in this study. In the method Zhang1, the time step used to obtain mass matrix is considered to be equal to one. In the procedure RPTH2, damping is determined based on the Zhang approach. Furthermore, the minimum residual force is used for time step in the mdDR2 method.

Table 1. Applied dynamic relaxation methods and their signs

Number	Method	Index
1	Papadrakakis	Papadrakakis
2	Underwood	Underwood
3	Qiang	Qiang
4	Zhang 1	Zhang 1
5	Zhang 2	Zhang 2
6	Nodal Damping	Nodal Damping
7	Rezaiee-Pajand & Taghavian Hakkak1	RPTH 1
8	Kinetic Dynamic Relaxation	kdDR
9	Minimizing the residual force	MFT
10	Rezaiee-Pajand & Alamatian1	mdDR 1
11	Rezaiee-Pajand & Alamatian2	mdDR 2

Number	Method	Index
12	Minimizing the residual Energy	MRE
13	Rezaiee-Pajand & Sarafrazi	RPS
14	Zero Damping	zdDR
15	Dunkerley	Dunkerley
16	Rezaiee-Pajand & Taghavian Hakkak2	RPTH 2

3.1 The quadrangle plate with various support conditions

The first example is a quadrangle plate on which the uniform distributed load applied. This structure is analyzed in three different states. Two types of these are square plates which one of these has the clamped supports and the other one is a simple support. The third one is a rectangular plate with the clamped supports and the ratio of length to width is equal to 2. Figure 1 shows the model of these structures. The width of plate (b) is equal to 1 m. The meshes used in the analyses were 10×10 and 20×20. Because of symmetry, a quarter of plate is modeled. The Figure 2 to Figure *4* indicate the maximum load-displacement graphs. The maximum deflection is occurred in the middle of the plate. In these figures, the load parameter is defined as a ratio $\frac{12qb^4\left(1-\upsilon^2\right)}{Eh^4}$. Here, the uniform load is assigned by q. The horizontal axis of load-displacement diagrams presents the ratio of deflection to thickness of plate. In addition, the number of DR iterations and the analysis duration are reported in Table 2 to Table 7.

First of all, the result of authors' program is the same as the responses of reference [1]. Based on the Table 3, the method MFT is not able to analyze the clamped-support square plate with 20×20 mesh. Thus, the rank of this approach is zero. In addition, the tactics of RPTH1 and RPTH2 cannot analyze the clamped-support rectangular plate. The obtained results show that the RPS and mdDR1 processes have behaved similarly. In other words, the number of required iterations to achieve the response is almost the same. As it was expressed in RPS procedure, the minimum eigenvalue, which is calculated by Rayleigh principle and power iteration method, is used to evaluate the damping. The mdDR technique uses the Rayleigh principle. On the other hand, the Eqs. (32) and (34), which are used to calculate the damping, are homological. Therefore, it is concluded that the minimum frequency obtained from Rayleigh principle is less than that which is achieved from power iteration method. It should be added that methods Qiang and Zhang1 are almost similar to mdDR1 and RPS. Because these methods use Rayleigh principle, too.

The results of clamped-supports rectangular plate illustrate that the efficiency of mdDR2 and MRE algorithms are the same. In these methods, the fictitious mass and damping are calculated by similar relations. If the Eq. (33) has no real answer, the time step which is evaluated in MRF approach is applied in MRE process. Therefore, it is concluded that the minimum of unbalanced

energy tactic is not suitable to calculate the time step in these plates. In other words, the residual force minimization has been used to find time step. Based on the achieved results, the nodal damping and Papadrakakis procedures are the most efficient and inefficient techniques to analyze this quadrangle plate. The Figure 2 to Figure *4* show that the number of meshes have not influence on the responses. Thus, one type of grid will be used for the other samples.

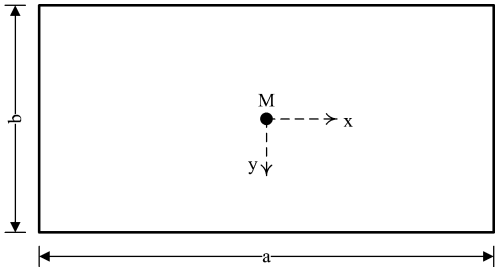

Figure 1. The rectangular plate

Table 2. The ranking of methods for the clamped-supports square plate (10X10 mesh)

Method	Total Iterations	Score	Grade	Time (Second)	Score	Grade
1	17438	0	16	3.578	0	16
2	3371	99.161	4	0.625	99.461	2
3	3721	96.694	11	0.734	95.79	9
4	3728	96.645	12	0.657	98.383	6
5	3909	95.369	14	0.703	96.834	8
6	3467	98.484	7	0.641	98.922	3
7	3353	99.288	3	0.656	98.417	4
8	4990	87.748	15	0.813	93.129	10
9	3412	98.872	6	0.859	91.58	12
10	3718	96.715	8	0.688	97.339	7
11	3252	100	1	0.844	92.085	11
12	3279	99.81	2	0.89	90.536	13
13	3719	96.708	9	1	86.831	14
14	3852	95.77	13	1.032	85.753	15
15	3720	96.701	10	0.657	98.383	6
16	3393	99.006	5	0.609	100	1

Table 3. The ranking of methods for the clamped-supports square plate (20X20 mesh)

Method	Total Iterations	Score	Grade	Time (Second)	Score	Grade
1	153621	0	15	616.922	0	15
2	12322	99.346	5	39.125	99.406	3
3	12912	98.931	10	47.156	98.024	9
4	12913	98.931	11	40.453	99.177	5
5	13544	98.487	13	41.985	98.914	7

Method	Total Iterations	Score	Grade	Time (Second)	Score	Grade
6	11392	100	1	35.781	99.981	2
7	12821	98.995	6	46.657	98.11	8
8	11450	99.959	2	35.672	100	1
9			0			0
10	12909	98.933	8	40.765	99.124	6
11	12303	99.359	4	54.078	96.833	10
12	12259	99.39	3	54.484	96.764	11
13	12910	98.933	9	63.828	95.156	13
14	13035	98.845	12	64.5	95.04	14
15	20540	93.568	14	63.234	95.258	12
16	12831	98.988	7	39.594	99.325	4

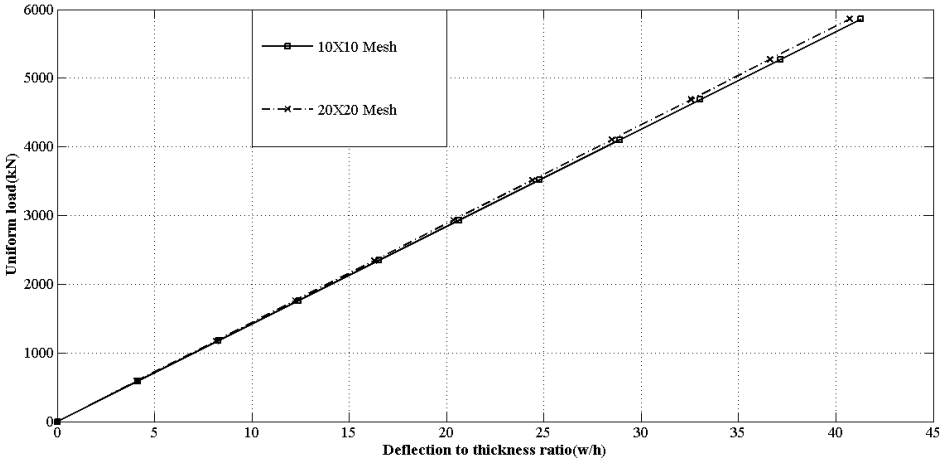

Figure 2. The load- maximum deflection curves for the clamped-supports square plate

Table 4. The ranking of methods for the clamped-supports rectangular plate (10X10 mesh)

Method	Total Iterations	Score	Grade	Time (Second)	Score	Grade
1	11393	0	13	2.375	0	14
2	3870	99.117	2	0.719	98.162	2
3	4387	92.306	7	0.828	91.701	6
4	4391	92.253	8	0.75	96.325	3
5	4604	89.447	10	0.812	92.65	5
6	3803	100	1	0.688	100	1
7			0			0
8	7110	56.43	12	1.079	76.823	9
9	3945	98.129	4	0.938	85.181	7
10	4383	92.358	5	0.765	95.436	4
11	3935	98.261	3	0.969	83.343	8
12	3935	98.261	3	1.094	75.934	10

Method	Total Iterations	Score	Grade	Time (Second)	Score	Grade
13	4384	92.345	6	1.157	72.199	11
14	4526	90.474	9	1.329	62.004	13
15	6900	59.196	11	1.188	70.362	12
16			0			0

Table 5. The ranking of methods for the clamped-supports rectangular plate (20X20 mesh)

Method	Total Iterations	Score	Grade	Time (Second)	Score	Grade
1	131065	0	12	525.797	0	14
2	13832	99.618	2	43.735	99.632	2
3	15488	98.21	5	56.219	97.052	6
4	15490	98.209	6	48.484	98.65	3
5	16246	97.566	9	50.438	98.246	5
6	13382	100	1	41.953	100	1
7			0			0
8	19140	95.107	10	58.703	96.538	7
9	15575	98.137	7	66.906	94.843	10
10	15487	98.211	4	49.109	98.521	4
11	15118	98.525	3	65.562	95.121	8
12	15118	98.525	3	66.75	94.875	9
13	15488	98.21	5	76.515	92.857	11
14	15621	98.097	8	77.484	92.657	12
15	34080	82.412	11	105.422	86.882	13
16			0			0

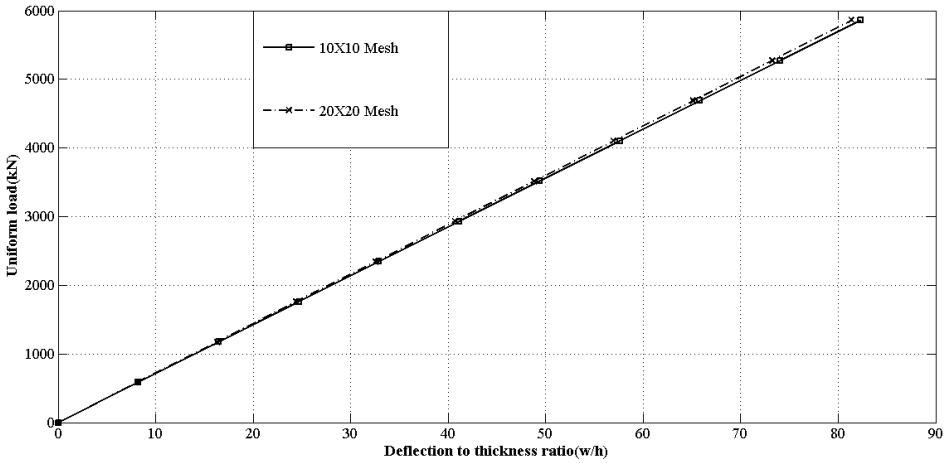

Figure 3. The load- maximum deflection curves for the clamped-supports rectangular plate

Table 6. The ranking of methods for the simple-supports square plate (10X10 mesh)

Method	Total Iterations	Score	Grade	Time (Second)	Score	Grade
1	15460	0	16	3.734	0	16
2	3393	100	1	0.687	99.025	3
3	3736	97.158	9	0.812	94.963	9
4	3738	97.141	10	0.703	98.505	5
5	3918	95.649	14	0.719	97.985	6
6	3517	98.972	4	0.703	98.505	5
7	3682	97.605	7	0.797	95.45	8
8	3630	98.036	5	0.657	100	1
9	3661	97.779	6	1.031	87.845	10
10	3745	97.083	11	0.735	97.465	7
11	3508	99.047	3	1.078	86.318	11
12	3506	99.064	2	1.079	86.285	12
13	3746	97.075	12	1.172	83.263	14
14	3820	96.461	13	1.171	83.295	13
15	8430	58.258	15	1.562	70.588	15
16	3694	97.506	8	0.672	99.513	2

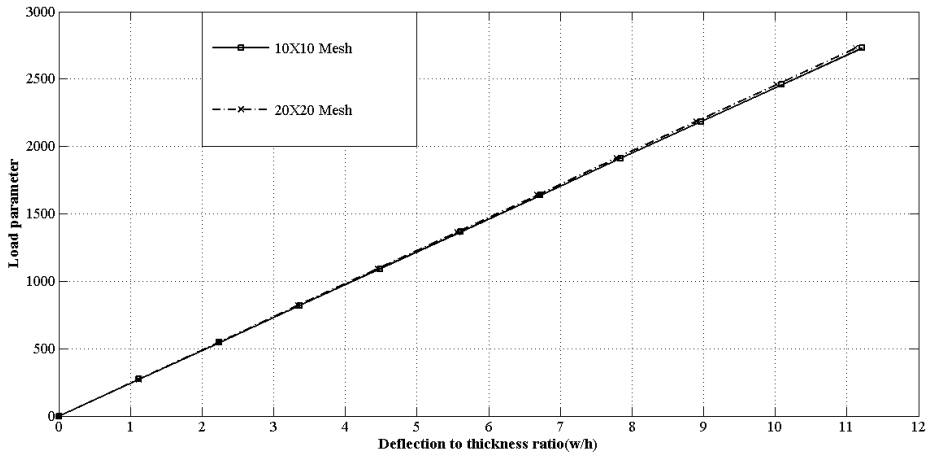

Figure 4. The load- maximum deflection curves for the simple-supports rectangular plate

Table 7. The ranking of methods for the simple-supports square plate (20X20 mesh)

Method	Total Iterations	Score	Grade	Time (Second)	Score	Grade
1	90342	0	15	434.797	0	16
2	13818	98.654	10	52.062	98.75	6
3	13422	99.165	5	58.297	97.141	8
4	13421	99.166	4	49.985	99.286	3
5	14081	98.315	13	52.313	98.685	7
6	12774	100	1	47.547	99.915	2
7	13846	98.618	11	60.328	96.617	9

Method	Total Iterations	Score	Grade	Time (Second)	Score	Grade
8	12830	99.928	2	47.218	100	1
9	13660	98.858	9	68.75	94.444	12
10	13423	99.163	6	50.797	99.077	5
11	13318	99.299	3	68.047	94.626	10
12	13318	99.299	3	68.516	94.505	11
13	13424	99.162	7	78.156	92.018	13
14	13496	99.069	8	79.375	91.703	14
15	42390	61.819	14	155.11	72.163	15
16	13849	98.614	12	50.719	99.097	4

3.2 Circular plate

The benchmark sample shown in Figure 5 is analyzed. Because of symmetry in loading and geometry of plate, a quarter of it is considered. To analyze this plate, 67 elements are used. The maximum deflection which occurs at the center of plate is equal to $\frac{(5+\upsilon)qb^4}{1024(1+\upsilon)D}$ [1]. The Flexural rigidity of plate is $D=\frac{Eh^3}{12(1-\upsilon^2)}$. The total load applied on the plate is equal to 915750.91575 Pa. The related maximum deflection is obtained to be 19.93 cm. The tolerance of this answer with the exact one is 0.12 percent. The results of analysis are inserted in Table 8. It is observed that the technique of Rezaiee-Pajand and Taghavian Hakkak has no capability to analyze this plate. In other words, this approach has been divergent since first step and the error of residue force increases up to infinity. Then, the computer program stops. Thus, the rank of these methods is zero. Here, the procedures of mdDR2 and MRE behave as the same, too. Also, the processes of RPS, mdDR, Qiang and Zhang1 are similar. The cause of this behavior was mentioned in the prior example. Based on the obtained results, the nodal damping and Papadrakakis method are the most efficient and inefficient tactic to analyze this plate.

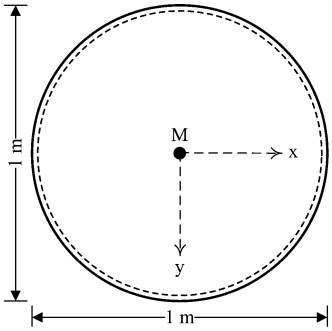

Figure 5. Circular plate

Table 8. The ranking of methods for the circular plate

Method	Total Iterations	Score	Grade	Time (Second)	Score	Grade
1	14502	0	16	119.25	0	16
2	3525	96.979	5	21.765	98.688	2
3	4031	92.508	10	30.344	90.003	11
4	4036	92.464	11	24.312	96.11	4
5	4231	90.741	13	25.656	94.749	6
6	3386	98.207	4	20.469	100	1
7	3701	95.424	6	27.532	92.85	10
8	5580	78.823	14	34.14	86.16	12
9	3306	98.913	3	27	93.388	9
10	4028	92.535	8	24.516	95.903	5
11	3183	100	1	25.797	94.606	7
12	3197	99.876	2	26.406	93.99	8
13	4029	92.526	9	41.047	79.168	14
14	4174	91.245	12	41.813	78.393	15
15	6110	74.141	15	37.078	83.186	13
16	3728	95.185	7	22.781	97.659	3

3.3 The rectangular plate with opening

Figure 6 shows the rectangular plate with the opening. Rezaiee-Pajand and Alamatian analyzed this structure [11]. The 20×20 mesh is used in this sample. The value of uniform load is equal to 915750.91575 N/m^2. The position of maximum deflection has been shown in Figure 6. The displacement of this node is equal to 8.306 cm in the final step. The responses are the same as results of reference [11].

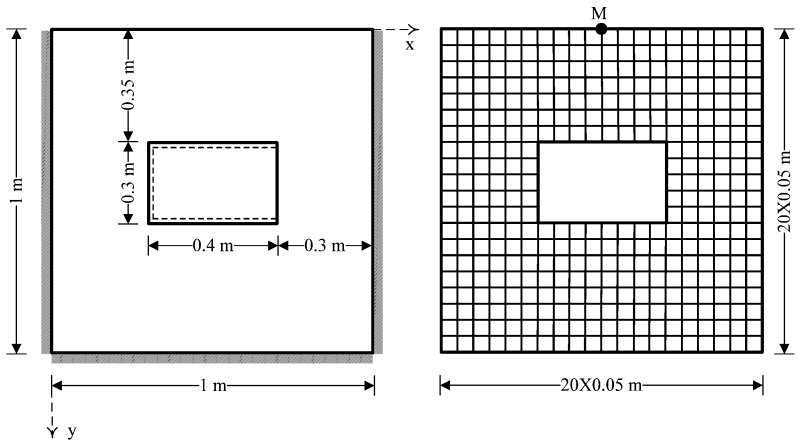

Figure 6. Rectangular plate with opening

The number of iterations and duration of analysis in each step of loading are presented in Table 9. Based on this, the methods of RPTH1 and RPTH2 have a

zero rank; because the responses of these tactics have been divergent. The most efficient approach to analyze this plate is the nodal damping algorithm. Also, the process of Papadrakakis has the highest time-consuming solution. The similarity of the procedures mdDR2 and MRE and also, the processes RPS, mdDR1, Qiang and Zhang1 is provided in this sample, too.

Table 9. The ranking of methods for the rectangular plate with opening

Method	Total Iterations	Score	Grade	Time (Second)	Score	Grade
1	73908	0	12	1297.234	0	14
2	9299	98.327	2	89.375	99.076	2
3	12258	93.824	6	153.938	93.78	11
4	12258	93.824	6	115.344	96.946	4
5	12858	92.911	10	121.688	96.425	6
6	11828	94.479	5	111.875	97.23	3
7			0			0
8	13420	92.056	11	127.578	95.942	9
9	10098	97.111	4	130.453	95.706	10
10	12274	93.8	7	116.969	96.812	5
11	9573	97.91	3	124.765	96.173	7
12	9573	97.91	3	125.859	96.083	8
13	12275	93.798	8	265.937	84.593	13
14	12443	93.543	9	263.344	84.806	12
15	8200	100	1	78.109	100	1
16			0			0

3.4 The L-shape plate

Here, the L-shaped plate illustrated in Figure 7 is analyzed with sixteen different processes of DR [8]. The uniform load applying in this plate is equal to 915750.91575 Pa. The boundary conditions along the edges are assigned with the number and symbol. The free edge, fixed and simple support are defined with F, C and S, respectively. For example, the CSCSSS plate has the clamped support in the edges 1 and 3, and the other supports are simple. The maximum deflection of CCCCCC and CSCSSS plate is happened at the point with the coordinates (0.5, 0.5). The value of this deflection is equal to 6.683 and 9.241 cm for CCCCCC and CSCSSS plate, correspondingly. This point is located at the middle of edge 2 for SFSSSF plate. The maximum displacement of this plate is equal to 57.35 cm. The ranking of methods is established in Table 10 to Table 12. The duration of analysis for Underwood and nodal damping procedures is less than others. In addition, the MRE and mdDR2 require a smaller number of iterations to achieve the response. It is mentioned that these two tactics show the same behavior. Based on the Table 11, the approach of Rezaiee-Pajand and Taghavian Hakkak cannot analyze the SFSSSF plate.

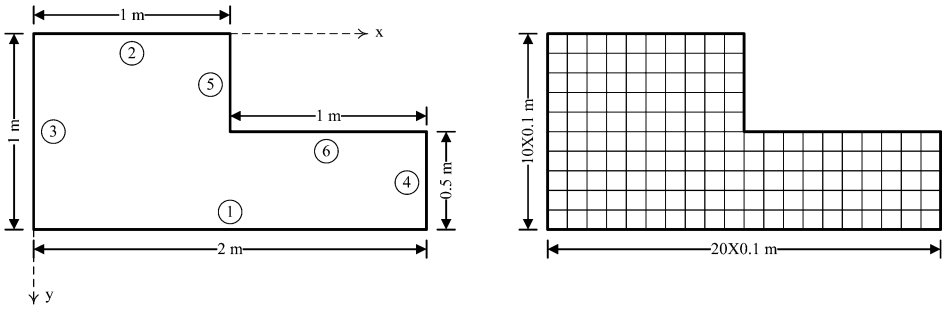

Figure 7. The L- shaped plate

Table 10. The ranking of methods for CCCCCC plate

Method	Total Iterations	Score	Grade	Time (Second)	Score	Grade
1	16791	0	15	188.422	0	16
2	4123	97.132	5	29.297	98.778	2
3	4799	91.949	8	42.156	90.795	12
4	4801	91.934	10	33.906	95.917	5
5	5033	90.155	12	34.953	95.267	6
6	3918	98.704	3	27.328	100	1
7	4539	93.943	6	39.859	92.221	10
8	5860	83.814	13	41.531	91.183	11
9	3966	98.336	4	37.11	93.928	9
10	4800	91.941	9	33.734	96.023	4
11	3770	99.839	2	35.547	94.898	8
12	3749	100	1	35.25	95.082	7
13	4801	91.934	10	66.125	75.917	15
14	4947	90.814	11	64.047	77.206	14
15	6710	77.296	14	46.781	87.924	13
16	4563	93.759	7	31.969	97.119	3

Table 11. The ranking of methods for SFSSSF plate

Method	Total Iterations	Score	Grade	Time (Second)	Score	Grade
1	184496	0	12	16243.969	0	14
2	13539	99.267	2	739.844	99.606	2
3	15924	97.882	7	1254.047	96.303	11
4	15925	97.882	8	863.016	98.815	5
5	16702	97.431	11	906.547	98.536	7
6	12277	100	1	678.593	100	1
7			0			0
8	14230	98.866	5	808.766	99.164	4
9	14790	98.541	6	1172.907	96.824	8
10	15925	97.882	8	878.187	98.718	6
11	13712	99.167	3	1200.485	96.647	9
12	13712	99.167	3	1208.359	96.597	10

Method	Total Iterations	Score	Grade	Time (Second)	Score	Grade
13	15926	97.881	9	2416.547	88.834	13
14	16072	97.796	10	2380.61	89.065	12
15	13790	99.121	4	746.781	99.562	3
16			0			0

Table 12. The ranking of methods for CSCSSS plate

Method	Total Iterations	Score	Grade	Time (Second)	Score	Grade
1	307499	0	13	435.312	0	14
2	27768	100	1	22.266	100	1
3	64506	86.867	7	74.172	87.433	6
4	64518	86.862	8	49.703	93.357	3
5	67660	85.739	10	51.625	92.892	4
6	195360	40.088	12	149.859	69.109	13
7			0			0
8	32230	98.405	2	24.11	99.554	2
9	61043	88.105	3	102.484	80.579	8
10	64478	86.877	6	52.938	92.574	5
11	63807	87.117	4	109.469	78.888	9
12	63807	87.117	4	112.735	78.097	10
13	64467	86.881	5	140.625	71.345	11
14	64909	86.723	9	142.75	70.83	12
15	119443	67.227	11	92.578	82.977	7
16			0			0

3.5 Triangular plate

A triangular plate is depicted in Figure 8. To analyze this structure, 60 elements are used. The uniform load 1831501.8315 N/m^2 is applied on the plate in ten steps. The maximum deflection occurs at the middle of the triangular.

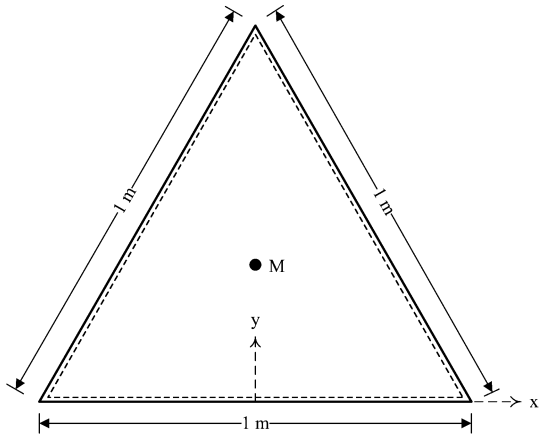

Figure 8. Triangular plate

The right answer is equal to $\frac{qa^4}{1728D}$ [1]. The length of each edge is defined with a. The value of 5.672 cm was obtained by the DR method. This quantity has 2 percent tolerance with the exact solution. Table 13 shows the results of analysis. Based on this, the minimum number of iterations is related to mdDR2 technique. In addition, the analysis duration for Zhang algorithm is the least. It should be added that the residual forces obtained in RPTH1 and RPTH2 processes exceed the allowable value. Therefore, the rank of these methods is zero. It is mentioned that the mdDR1 and RPS tactics have the same number of iterations.

Table 13. The ranking of methods for the triangular plate

Method	Total Iterations	Score	Grade	Time (Second)	Score	Grade
1	296610	0	12	234.219	0	14
2	24264	98.416	2	11.5	98.705	2
3	25669	97.908	5	16.75	96.378	7
4	25668	97.908	4	11.672	98.629	3
5	26923	97.455	9	12.156	98.414	4
6	27557	97.226	10	12.843	98.11	6
7			0			0
8	19880	100	1	8.578	100	1
9	26336	97.667	8	25.125	92.667	9
10	25680	97.904	6	12.375	98.317	5
11	25281	98.048	3	24.375	92.999	8
12	25281	98.048	3	25.765	92.383	10
13	25680	97.904	6	29.937	90.534	11
14	25794	97.863	7	29.938	90.534	12
15	123934	62.399	11	55.594	79.163	13
16			0			0

3.6 Parallelogram plate

Moreover, the analysis of parallelogram plate is presented. This structure and its meshing are illustrated in Figure 9. The value of uniform load applied on the plate is equal to 183150.18315 Pa. The ranking of approaches is reported in Table 14. In this sample, Rezaiee-Pajand and Taghavian Hakkak process cannot obtain the correct answer. In other words, the residual force tends to infinity and divergent. On the other hand, the procedures of nodal damping, kinetic DR and Underwood are the first to third ranks respectively in the number of iteration and duration of analysis to achieve the acceptable error. It is mentioned that mdDR2 and MRE methods and also RPS, mdDR1, Qiang and Zhang1 tactics have the same behavior in the number of iterations. It should be added that the maximum deflection value is equal to 42.47 cm.

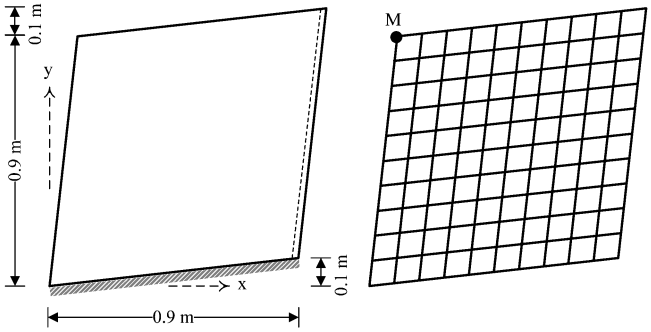

Figure 9. Parallelogram plate

Table 14. The ranking of methods for the parallelogram plate

Method	Total Iterations	Score	Grade	Time (Second)	Score	Grade
1	452071	0	12	519.141	0	14
2	21271	99.69	8	13.844	99.704	4
3	21158	99.716	4	19.938	98.502	7
4	21158	99.716	4	13.562	99.76	3
5	22189	99.477	10	14.047	99.664	5
6	19930	100	1	12.782	99.914	2
7			0			0
8	20470	99.875	3	12.344	100	1
9	21752	99.578	9	29.812	96.553	10
10	21159	99.716	5	14.125	99.649	6
11	20383	99.895	2	28.547	96.803	8
12	20383	99.895	2	29.797	96.556	9
13	21160	99.715	6	36.812	95.172	11
14	21265	99.691	7	37.797	94.978	12
15	84300	85.104	11	52.188	92.138	13
16			0			0

3.7 The irregular tetrahedron plate I

In this section, the different processes of DR are studied in the analysis of plate shown in Figure 10. In this analysis, 233 bending plate elements are applied. This structure is subjected to uniform load 1831501.8315 N/m^2. The maximum deflection is located at the node M which has a coordinate (0.24, 0.42). This value is equal to 7.972 cm. The ranking of used techniques are established in Table 15. Based on this table, the methods RPTH1 and RPTH2 cannot analyze this plate. Underwood process is the best approach. Also, RPS and mdDR1 procedures behave similarly. These tactics are almost the same as the Zhang1 and Qiang solutions.

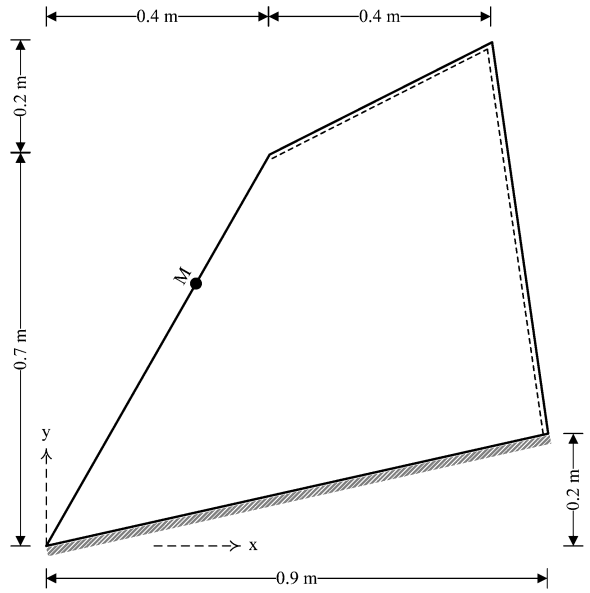

Figure 10. The irregular tetrahedron plate I

Table 15. The ranking of methods for the irregular tetrahedron plate I

Method	Total Iterations	Score	Grade	Time (Second)	Score	Grade
1	269118	37.965	10	1809.234	16.502	13
2	47283	95.557	6	245.375	95.339	4
3	46675	95.715	3	283.969	93.394	7
4	46676	95.715	4	240.906	95.565	3
5	48956	95.123	8	249.438	95.134	5
6	51542	94.451	9	264.828	94.359	6
7			0			0
8	30170	100	1	152.921	100	1
9	48493	95.243	7	330.687	91.038	10
10	46675	95.715	3	240.859	95.567	2
11	46511	95.758	2	317.797	91.688	8
12	46511	95.758	2	322.641	91.444	9
13	46675	95.715	3	390.281	88.034	12
14	46773	95.69	5	385.328	88.284	11
15	415350	0	11	2136.578	0	14
16			0			0

3.8 The irregular tetrahedron plate II

Another quadrangle plate is analyzed. The geometry of this structure is shown in Figure 11. The applied load on this plate is equal to 915750.91575 Pa. Maximum deflection is located at the middle of free edge. The value of that is equal to 8.255 cm. The obtained results are reported in Table 16. This table

shows the inefficiency of Rezaiee-Pajand and Taghavian Hakkak method. It should be added that the methods of RPS, mdDR1, Zhang1 and Qiang have the same number of iterations to achieve the response in each growth of loading. In other words, these methods have behaved homologically.

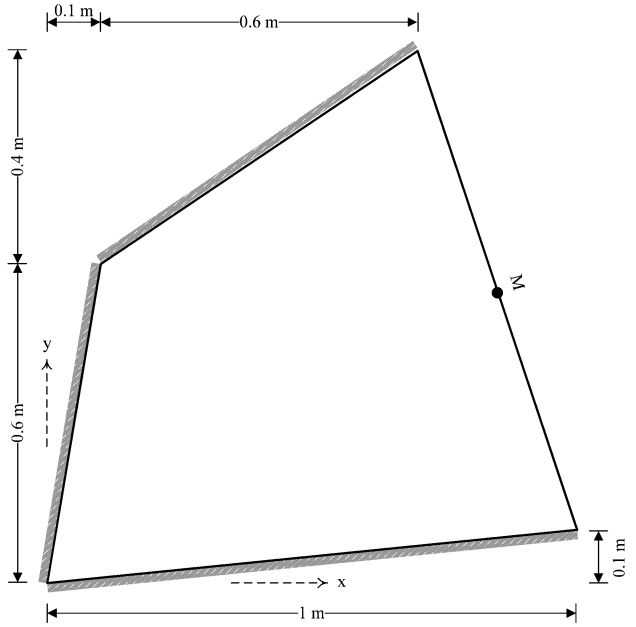

Figure 11. The irregular tetrahedron plate II

Table 16. The ranking of methods for the irregular tetrahedron plate II

Method	Total Iterations	Score	Grade	Time (Second)	Score	Grade
1	88560	0	13	51.203	0	14
2	10666	98.394	10	3.875	98.89	5
3	9950	99.299	3	4.641	97.29	7
4	9952	99.296	4	3.469	99.739	2
5	10435	98.686	9	3.61	99.444	3
6	9395	100	1	3.344	100	1
7			0			0
8	11480	97.366	11	3.937	98.761	6
9	10075	99.141	8	6.953	92.459	9
10	9961	99.285	5	3.625	99.413	4
11	9756	99.544	2	6.781	92.818	8
12	9756	99.544	2	7.172	92.002	10
13	9962	99.284	6	8.031	90.207	11
14	10069	99.149	7	8.063	90.14	12
15	27510	77.117	12	9.484	87.171	13
16			0			0

3.9 Elliptical plate

In this section, the elliptical plate shown in Figure 12 is analyzed. The uniform load is equal to 915750.91575 N/m^2. Because of symmetry, a quarter of plate is modeled with 44 elements. The maximum deflection occurs at the center of the plate. Timoshenko was obtained the exact solution equal to $\frac{1.58qb^4}{Eh^3}$ [1]. The small radius of ellipsoid is *b*. The scores of processes are inserted in Table 17. Among the convergent methods, the nodal damping algorithm is the best solution and the Papadrakakis process is the worst one. The residue force error in Rezaiee-Pajand and Taghavian Hakkak tactic increases successive. In other words, this approach is inefficient to analyze this plate. On the other hand, the RPS and mdDR1 techniques behave similarly. In addition, the number of iterations is the same in MRE and mdDR2 for each increment loading. Also, Qiang and Zhang1 procedures are similar. It is mentioned that the maximum deflection is equal to 44.76 cm. The tolerance of this value with the exact response is 1 percent.

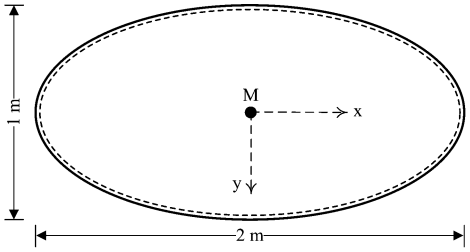

Figure 12. The elliptical plate

Table 17. The ranking of methods for the elliptical plate

Method	Total Iterations	Score	Grade	Time (Second)	Score	Grade
1	349986	0	12	13664.641	0	14
2	15199	99.268	2	341.515	99.536	2
3	19517	97.988	7	614	97.501	7
4	19517	97.988	7	440.407	98.798	4
5	20468	97.706	9	456.891	98.674	5
6	32704	94.077	11	732.063	96.619	11
7			0			0
8	20740	97.625	10	471.485	98.565	6
9	19308	98.05	4	651.953	97.217	10
10	19512	97.989	5	431.328	98.865	3
11	18751	98.215	3	635.281	97.342	9
12	18751	98.215	3	632.968	97.359	8
13	19514	97.988	6	1102.281	93.853	12
14	19677	97.94	8	1111.265	93.786	13
15	12730	100	1	279.469	100	1
16			0			0

3.10 The donut-shaped plate

In this example, the plate illustrated in Figure 13 is investigated. The uniform load is equal to 183150.18315 Pa. Because of symmetry, a quarter of plate is modeled by 90 elements. Table 18 shows the responses. For this structure, the most efficient method is kdDR. In other words, this solution requires the least number of iteration and duration of analysis to achieve the response. The RPTH1 and RPTH2 procedures cannot analyze this plate. In addition, the processes RPS, mdDR1, Qiang and Zhang1 behave similarly. It should be added that MRE and mdDR2 is also the same. Furthermore, the maximum deflection is equal to 61.26 cm.

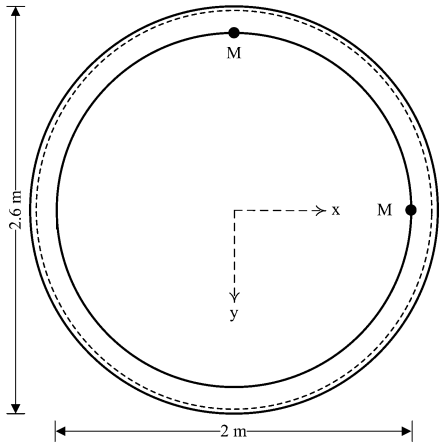

Figure 13. The donut-shaped plate

Table 18. The ranking of methods for the donut-shaped plate

Method	Total Iterations	Score	Grade	Time (Second)	Score	Grade
1	242068	0	12	1355.297	0	14
2	18094	98.589	3	76.25	98.905	3
3	18897	98.235	5	93.093	97.603	7
4	18898	98.235	6	78.625	98.722	4
5	19820	97.829	10	81.688	98.485	6
6	14888	100	1	62.093	100	1
7			0			0
8	17740	98.745	2	72.531	99.193	2
9	19481	97.978	9	113.796	96.002	10
10	18898	98.235	6	79.594	98.647	5
11	18609	98.362	4	108.437	96.416	8
12	18609	98.362	4	108.734	96.393	9
13	18899	98.234	7	131.781	94.611	11
14	19007	98.187	8	133.25	94.498	12
15	63910	78.422	11	261.297	84.596	13
16			0			0

3.11 The plate with arched-shape edges

Now, the structure shown in Figure 14 is analyzed. The right edge is a sector of circle with the radius of 0.5 m and the left edge is a three-point arch. In this model, 74 elements are used. The value of distributed load is equal to 915750.91575 N/m^2. The maximum deflection is occurred at the point with the coordinates (0, -0.25). This value is equal to 76.26 cm. the results are expressed in Table 19. Similar to recent samples, the method of Rezaiee-Pajand and Taghavian Hakkak cannot achieve to responses. The most efficient of techniques is Underwood process and the worst one is Papadrakakis algorithm. It is mentioned that the MRE and mdDR2 approaches have behaved the same.

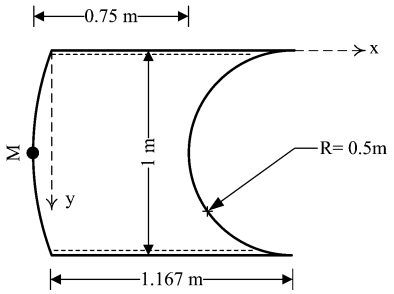

Figure 14. The plate with arched-shape edges

Table 19. The ranking of methods for the plate having with arched-shape edges

Method	Total Iterations	Score	Grade	Time (Second)	Score	Grade
1	306931	0	14	14855.313	0	14
2	14220	100	1	393.562	100	1
3	16347	99.273	8	637.156	98.316	9
4	16346	99.274	7	449.031	99.616	5
5	17146	99	12	470.39	99.469	6
6	15664	99.507	4	432.375	99.732	2
7			0			0
8	20540	97.841	13	575.547	98.742	7
9	16097	99.359	6	674.078	98.06	11
10	16361	99.269	9	444.844	99.645	4
11	14965	99.745	2	628.641	98.374	8
12	15009	99.73	3	641.437	98.286	10
13	16362	99.268	10	1149.531	94.773	12
14	16493	99.223	11	1189.594	94.496	13
15	16030	99.382	5	433.5	99.724	3
16			0			0

3.12 The circular plate with rectangular opening

The plate illustrated in Figure 15 is considered. The uniform load is equal to 1831501.8315 Pa. This structure is symmetric. Therefore, a quarter of that is

considered to grid. In this plate, 52 elements are used. The number of iterations and analysis duration are inserted in Table 20. The results related to this example are almost the same as the responses obtained in donut shaped plate. It should be added that the maximum deflection is equal to 58.03 cm.

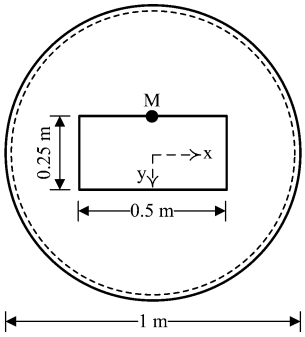

Figure 15. The circular plate with rectangular opening

Table 20. The ranking of methods for the circular plate with rectangular opening

Method	Total Iterations	Score	Grade	Time (Second)	Score	Grade
1	59720	0	14	280.234	0	14
2	5519	99.761	3	21.641	99.879	2
3	6172	98.559	8	27.39	97.659	6
4	6173	98.557	9	23.781	99.053	4
5	6474	98.003	11	24.453	98.793	5
6	5556	99.693	4	21.329	100	1
7			0			0
8	9260	92.875	13	35	94.72	11
9	5558	99.689	5	28.5	97.23	10
10	6168	98.566	6	23.718	99.077	3
11	5414	99.954	2	28	97.423	9
12	5389	100	1	27.907	97.459	8
13	6170	98.563	7	36.782	94.031	12
14	6293	98.336	10	37.281	93.839	13
15	7220	96.63	12	27.469	97.628	7
16			0			0

3.13 The L-shaped plate with opening

The plate shown in Figure 16 is analyzed with 16 different methods. In this figure, the values of *a* and *b* are equal to 0.3 and 0.2, respectively. This structure is subjected to uniform load 183150.18315 N/m^2. It is reminded that this plate without any opening was previously analyzed. The maximum deflection occurs in the node with the coordinates (1.4, 0.5). The maximum displacement is equal to 4.916 cm. To analyze this plate, 199 bending elements are used. The obtained results are established in Table 21. The tolerance of residual force tends to

infinity for Rezaiee-Pajand and Taghavian Hakkak method. Thus, the response of this procedure is divergent and the rank of that is zero. In addition, the number of iterations is the same for mdDR2 and MRE processes. Therefore, these tactics have behaved similarly. The Qiang, Zhang1, RPS and mdDR1 approaches are also the same. It is mentioned that the Dunkerley and Underwood techniques have the first and second rank, respectively.

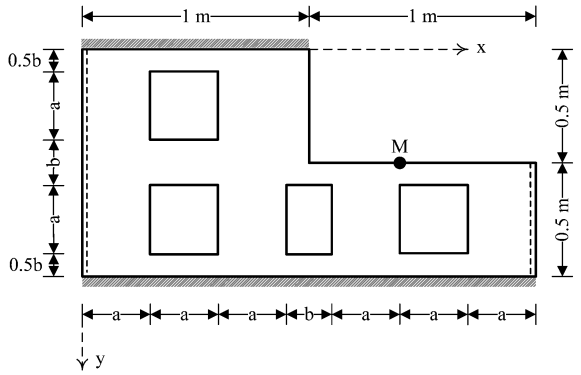

Figure 16. The L-shaped plate with opening

Table 21. The ranking of methods for the L-shaped plate with opening

Method	Total Iterations	Score	Grade	Time (Second)	Score	Grade
1	342661	0	12	1287.875	0	14
2	40926	99.408	2	114.031	99.361	2
3	46155	97.686	6	152.109	96.138	7
4	46154	97.686	5	128.422	98.143	4
5	48405	96.944	10	133.079	97.749	6
6	43312	98.622	3	119.266	98.918	3
7			0			0
8	39130	100	1	106.484	100	1
9	48094	97.047	9	188.672	93.043	10
10	46156	97.685	7	129.469	98.054	5
11	45811	97.799	4	180.234	93.757	8
12	45811	97.799	4	180.906	93.7	9
13	46155	97.686	6	221.203	90.289	12
14	46294	97.64	8	221.031	90.304	11
15	242801	32.899	11	664.515	52.765	13
16			0			0

3.14 The rectangular plate with circular opening

Figure 17 shows the rectangular plate with circular opening. The value of uniform load applied on the structure is equal to 915750.91575 Pa. Because of symmetry, a quarter of plate with 76 elements is modeled. The ranking of

methods is reported in Table 22. Based on the Table 22, the RPTH1 and RPTH2 tactics cannot achieve to the response. It should be added that the mdDR2 and MRE processes and also Qiang, Zhang1, RPS and mdDR1 have behaved similarly. The kinetic damping algorithm has the highest rate of convergence. The Underwood approach is located at the next rank. The ratio of maximum deflection to thickness is obtained to be equal to 83.18.

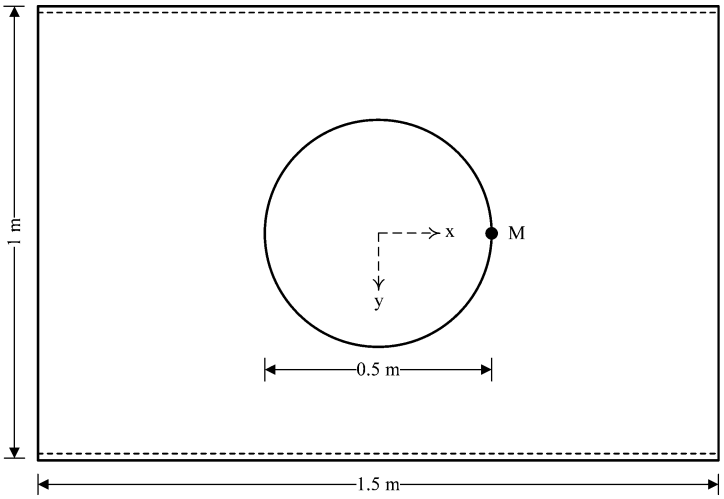

Figure 17. The rectangular plate with circular opening

Table 22. The ranking of methods for the rectangular plate with circular opening

Method	Total Iterations	Score	Grade	Time (Second)	Score	Grade
1	191397	0	12	1195.859	0	14
2	14824	99.863	2	73.344	99.85	2
3	15493	99.485	6	90.078	98.361	7
4	15493	99.485	6	75.5	99.658	4
5	16246	99.059	10	79.156	99.333	6
6	14582	100	1	71.656	100	1
7			0			0
8	15590	99.43	7	75.11	99.693	3
9	15784	99.32	9	102.094	97.292	10
10	15491	99.486	4	76.031	99.611	5
11	14937	99.799	3	97.61	97.691	8
12	14937	99.799	3	97.969	97.659	9
13	15492	99.485	5	121.125	95.6	11
14	15594	99.428	8	121.688	95.55	12
15	37940	86.79	11	184.062	90.001	13
16			0			0

3.15 The quarter of donut

The structure in Figure 18 is investigated. The plate is modeled by 90 bending plate elements. The uniform load is equal to 183150.18315 N/m^2. The maximum deflection happens at the middle of internal edge. This value is equal to 7.064 cm. Table 23 shows the number of iterations and analysis duration. The obtained responses are almost the same as the previous sample. But here, the nodal damping has the first rank.

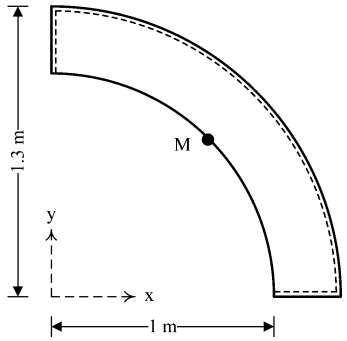

Figure 18. The quarter of donut plate

Table 23. The ranking of methods for the quarter of donut

Method	Total Iterations	Score	Grade	Time (Second)	Score	Grade
1	334152	0	12	2647.312	0	14
2	37422	99.579	2	223.328	99.629	2
3	38989	99.053	4	283.156	97.17	7
4	38989	99.053	4	229.875	99.36	3
5	40891	98.414	10	240.797	98.911	6
6	36166	100	1	214.297	100	1
7			0			0
8	39410	98.911	8	230.641	99.328	5
9	40640	98.499	9	321.563	95.591	10
10	38996	99.05	5	230.359	99.34	4
11	38729	99.14	3	305.422	96.255	8
12	38729	99.14	3	307.985	96.149	9
13	38997	99.05	6	379.14	93.225	11
14	39114	99.011	7	379.829	93.196	12
15	235922	32.965	11	1397.156	51.383	13
16			0			0

3.16 The quarter of circular plate

The final sample is the quarter of circular plate. Figure 19 illustrates the geometry of structure. The modeling is performed by 113 elements. The applied load is equal to 183150.8315 Pa. the maximum deflection is located at the central node of external boundary. The results are inserted in Table 24. The

ranking of techniques is almost the same as the previous sample. The ratio of maximum deflection to thickness is achieved to be equal to 632.7.

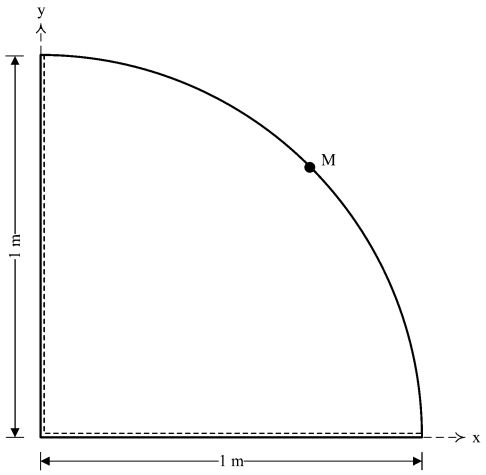

Figure 19. The quarter of circular plate

Table 24. The ranking of methods for the quarter of circular plate

Method	Total Iterations	Score	Grade	Time (Second)	Score	Grade
1	32713	0	14	31.984	0	14
2	4047	98.482	10	2.437	99.264	4
3	3810	99.296	3	3.14	96.903	6
4	3816	99.275	4	2.218	100	1
5	4000	98.643	9	2.297	99.735	2
6	5361	93.967	11	3.094	97.057	5
7			0			0
8	5930	92.013	13	3.312	96.325	8
9	3717	99.615	2	4.391	92.7	10
10	3829	99.23	5	2.313	99.681	3
11	3605	100	1	4.344	92.858	9
12	3918	98.925	7	4.844	91.178	11
13	3830	99.227	6	5.656	88.45	12
14	3949	98.818	8	5.844	87.818	13
15	5620	93.078	12	3.218	96.64	7
16			0			0

4 THE RANKING OF METHODS

Based on the results of each sample, a rank among one to sixteen is assigned to each approach. The rank one shows the best tactic whereas the rank sixteen indicates the worst one. The ranks j can be counted for method i and Q_{ij} is found. For instance, according to number of iterations, the MRE is ranked third

for eleven times. Therefore, the value of Q_{i3} for this process is equal to eleven. The value of Q_{i0} shows the number of structures on which the procedure *i* cannot be applied. Based on the values of Q_{ij}, the score of schemes *i* is obtained as follow:

$$S_{ij} = 100 \times \sum_{j=1}^{16} Q_{ij} \times (17 - j) / 368 \tag{42}$$

It should be added that when a method gains the first rank in all 23 examples, the score 368 is obtained. As a result, the score S_{ij} for this method will be equal to 100. The number of ranks and scores are reported in Table 25 and Table 26. It should be mentioned that if an approach has not an ability to achieve the response, it is not considered in Eq. (42).

Table 25. The ranking of methods based on the number of iterations

Grade	Score	Method	Q_{ij}																
			0	1	2	3	4	5	6	7	8	9	10	11	12	13	14	15	16
1	89.6739	11	0	3	6	10	4	0	0	0	0	0	0	0	0	0	0	0	0
2	88.3152	12	0	2	6	11	3	0	0	1	0	0	0	0	0	0	0	0	0
3	81.7935	2	0	3	9	2	1	3	1	0	1	0	3	0	0	0	0	0	0
4	79.8913	6	0	10	0	2	4	1	0	1	0	1	1	2	1	0	0	0	0
5	66.5761	10	0	0	0	1	2	6	5	2	4	2	0	1	0	0	0	0	0
6	66.3043	3	0	0	0	3	2	4	3	4	3	1	2	1	0	0	0	0	0
7	64.4022	9	1	0	1	2	4	1	4	2	2	6	0	0	0	0	0	0	0
8	63.3152	4	0	0	0	0	7	1	4	2	3	1	2	2	1	0	0	0	0
9	61.9565	13	0	0	0	1	0	3	8	3	1	4	2	0	1	0	0	0	0
10	58.9674	8	0	3	4	1	0	2	0	1	1	0	2	2	1	4	1	1	0
11	49.7283	14	0	0	0	0	0	1	0	4	7	3	2	2	2	2	0	0	0
12	41.3043	15	0	2	0	0	1	1	0	0	0	0	1	10	3	0	3	2	0
13	39.4022	5	0	0	0	0	0	0	0	0	1	5	8	2	2	3	2	0	0
14	23.6413	1	0	0	0	0	0	0	0	0	0	0	1	0	10	3	3	3	3
15	17.1196	7	17	0	0	1	0	0	3	1	0	0	0	1	0	0	0	0	0
16	15.2174	16	17	0	0	0	0	1	0	3	1	0	0	0	1	0	0	0	0

Table 26. The ranking of methods based on the duration of analysis

Grade	Score	Method	Q_{ij}																
			0	1	2	3	4	5	6	7	8	9	10	11	12	13	14	15	16
1	89.9457	2	0	2	13	3	3	1	1	0	0	0	0	0	0	0	0	0	0
2	86.413	6	0	10	4	3	0	2	2	0	0	0	0	1	0	1	0	0	0
3	82.8804	4	0	1	1	8	7	5	1	0	0	0	0	0	0	0	0	0	0
4	77.1739	10	0	0	1	3	6	8	3	2	0	0	0	0	0	0	0	0	0
5	73.913	8	0	7	2	1	1	1	2	2	1	2	1	2	1	0	0	0	0
6	72.0109	5	0	0	1	1	2	6	9	3	1	0	0	0	0	0	0	0	0
7	56.7935	3	0	0	0	0	0	0	5	9	1	4	0	3	1	0	0	0	0
8	52.7174	11	0	0	0	0	0	0	0	2	12	5	2	2	0	0	0	0	0
9	46.4674	12	0	0	0	0	0	0	0	1	4	7	6	3	1	1	0	0	0
10	43.4783	9	1	0	0	0	0	0	0	1	2	4	12	1	2	0	0	0	0
11	42.9348	15	0	2	0	2	0	0	1	3	0	0	0	0	2	10	1	2	0

Grade	Score	Method	Q_{ij}																
			0	1	2	3	4	5	6	7	8	9	10	11	12	13	14	15	16
12	30.163	13	0	0	0	0	0	0	0	0	0	0	0	9	6	4	3	1	0
13	26.9022	14	0	0	0	0	0	0	0	0	0	0	0	2	10	6	3	2	0
14	23.0978	16	17	1	1	2	2	0	0	0	0	0	0	0	0	0	0	0	0
15	16.0326	1	0	0	0	0	0	0	0	0	0	0	0	0	0	1	16	1	5
16	14.4022	7	17	0	0	0	1	0	0	0	2	1	2	0	0	0	0	0	0

5 CONCLUSION

In this paper, a comparison study was performed between sixteen well-known methods of dynamic relaxation for elastic analysis of bending plates. First, the dynamic relaxation procedure and its formulations were defined. Then, the previous algorithms were expressed. Moreover, several samples were analyzed with linear behavior. The ranking of approaches was found based on the number of iteration and duration of analysis in each example. Based on this study, Rezaiee-Pajand and Alamatian scheme, which obtains the time step with minimum residual force tactic, have the least number of iterations to achieve the response. The short mark of this technique was mdDR2. It should be added that minimum unbalanced energy (MRE) and Underwood processes are ranked as sequent. In addition, according to analysis duration, the Underwood, nodal damping and Zhang methods were ranked first to third, respectively. On the other hand, the Rezaiee-Pajand and Taghavian-Hakak procedure was the most inefficient solution; because they used higher order approximations. Accordingly, this approach was divergent at seventeen samples. Also, among the convergent methods, the Papadrakakis process required the maximum number of iteration and duration of analysis to achieve the target accuracy. Furthermore, in the most of the analyses, the mdDR2 and MRE techniques, and also of Qiang, Zhang, RPS and mdDR1 schemes had similar behavior. In other words, the number of iterations for these methods was almost the same.

REFERENCES

[1] Timoshenko S, Woinowsky-Krieger S. Theory of plates and shells New York: McGraw-hill; 1959.

[2] Szilard R. Theories and applications of plate analysis: classical numerical and engineering methods New Jersey, USA: John Wiley & Sons; 2004.

[3] Day AS. "An introduction to dynamic relaxation". The Engineer, Vol. 219, No pp. 218-21, 1965.

[4] Otter JRH. "Computations for prestressed concrete reactor pressure vessels using dynamic relaxation". Nuclear Structural Engineering, Vol. 1, No 1, pp. 61-75, 1965.

[5] Otter JRH, Day AS. "Tidal computations". The Engineer Vol. 289, No pp. 177-82, 1960.

[6] Frankel SP. "Convergence rates of iterative treatments of partial differential equations". Mathematical Tables and Other Aids to Computation, Vol. 4, No 30, pp. 65–75, 1950.

[7] Rezaiee-Pajand M, Taghavian Hakkak M. "Nonlinear analysis of truss structures using dynamic relaxation". International Journal of Engineering, Vol. 19, No 1, pp. 11-22, 2006.

[8] Kadkhodayan M, Alamatian J, Turvey GJ. "A new fictitious time for the dynamic relaxation (DXDR) method". International Journal for Numerical Methods in Engineering, Vol. 74, No

6, pp. 996-1018, 2008.
[9] Rezaiee-Pajand M, Alamatian J. "Nonlinear dynamic analysis by dynamic relaxation method". Structural Engineering & Mechanics, Vol. 28, No 5, pp. 549-70, 2008.
[10] Rezaiee-Pajand M, Sarafrazi SR. "Nonlinear structural analysis using dynamic relaxation method with improved convergence rate". International Journal of Computational Methods, Vol. 7, No 4, pp. 627-54, 2010.
[11] Rezaiee-Pajand M, Alamatian J. "The dynamic relaxation method using new formulation for fictitious mass and damping". Structural Engineering and Mechanics, Vol. 34, No 1, pp. 109-33, 2010.
[12] Rezaiee-Pajand M, Kadkhodayan M, Alamatian J, Zhang LC. "A new method of fictitious viscous damping determination for the dynamic relaxation method". Comput Struct, Vol. 89, No 9–10, pp. 783-94, 2011.
[13] Rezaiee-Pajand M, Sarafrazi SR. "Nonlinear dynamic structural analysis using dynamic relaxation with zero damping". Comput Struct, Vol. 89, No 13–14, pp. 1274-85, 2011.
[14] Rezaiee-Pajand M, Kadkhodayan M, Alamatian J. "Timestep selection for dynamic relaxation method". Mechanics Based Design of Structures and Machines, Vol. 40, No 1, pp. 42-72, 2012.
[15] Alamatian J. "A new formulation for fictitious mass of the Dynamic Relaxation method with kinetic damping". Comput Struct, Vol. 90–91, No pp. 42-54, 2012.
[16] Rezaiee-Pajand M, Sarafrazi SR, Rezaiee H. "Efficiency of dynamic relaxation methods in nonlinear analysis of truss and frame structures". Comput Struct, Vol. 112–113, No 0, pp. 295-310, 2012.
[17] Rezaiee-Pajand M, Rezaee H. "Fictitious time step for the kinetic dynamic relaxation method". Mechanics of Advanced Materials and Structures, Vol. 21, No 8, pp. 631-44, 2012.
[18] Rezaiee-Pajand M, Estiri H. "A comparison of large deflection analysis of bending plates by dynamic relaxation". Periodica Polytechnica Civil Engineering, Vol. 60, No 4, pp. 619-45, 2016.
[19] Rezaiee-Pajand M, Estiri H. "Comparative analysis of three-dimensional frames by dynamic relaxation methods". Mechanics of Advanced Materials and Structures, Vol., No pp. 1-16, 2017.
[20] Rezaiee-Pajand M, Estiri H. "Geometrically nonlinear analysis of shells by various dynamic relaxation methods". World Journal of Engineering, Vol. 14, No 5, pp. 381-405, 2017.
[21] Rezaiee-Pajand M, Estiri H, Mohammadi-Khatami M. "Creating better dynamic relaxation methods". Engineering Computations, Vol. 36, No 5, pp. 1483-521, 2019.
[22] Lee K-S, Han S-E, Hong J-W. "Post-buckling analysis of space frames using concept of hybrid arc-length methods". International Journal of Non-Linear Mechanics, Vol. 58, No 0, pp. 76-88, 2014.
[23] Rezaiee-Pajand M, Estiri H. "Computing the structural buckling limit load by using dynamic relaxation method". International Journal of Non-Linear Mechanics, Vol. 81, No pp. 245-60, 2016.
[24] Rezaiee-Pajand M, Estiri H. "Mixing dynamic relaxation method with load factor and displacement increments". Comput Struct, Vol. 168, No pp. 78-91, 2016.
[25] Rezaiee-Pajand M, Estiri H. "Finding equilibrium paths by minimizing external work in dynamic relaxation method". Applied Mathematical Modelling, Vol. 40, No 23–24, pp. 10300-22, 2016.
[26] Rezaiee-Pajand M, Estiri H. "Finding buckling points for nonlinear structures by dynamic relaxation scheme". Frontiers of Structural and Civil Engineering, Vol. 14, No 1, pp. 23-61, 2020.
[27] Rezaiee-Pajand M, Alamatian J, Rezaee H. "The state of the art in Dynamic Relaxation methods for structural mechanics Part 1: Formulations". Iranian Journal of Numerical Analysis and Optimization, Vol. 7, No 2, pp. 65-86, 2017.

[28] Rezaiee-Pajand M, Alamatian J, Rezaee H. "The state of the art in Dynamic Relaxation methods for structural mechanics Part 2: Applications". Iranian Journal of Numerical Analysis and Optimization, Vol. 7, No 2, pp. 87-114, 2017.
[29] Shoukry SN, William GW, Riad MY, McBride KC. "Dynamic relaxation: A technique for detailed thermo-elastic structural analysis of transportation structures". International Journal for Computational Methods in Engineering Science and Mechanics, Vol. 7, No 4, pp. 303-11, 2006.
[30] Bagrianski S, Halpern AB. "Form-finding of compressive structures using Prescriptive Dynamic Relaxation". Comput Struct, Vol. 132, No pp. 65-74, 2014.
[31] Bel Hadj Ali N, Sychterz AC, Smith IFC. "A dynamic-relaxation formulation for analysis of cable structures with sliding-induced friction". International Journal of Solids and Structures, Vol. 126-127, No pp. 240-51, 2017.
[32] Met M, Wang G, Topa A. "The analysis on dynamic responses of bridge pier due to vehicle impact". American Journal of Engineering Research, Vol. 11, No pp. 169-81, 2022.
[33] Golmakani ME, Zeighami V. "Nonlinear thermo-elastic bending of functionally graded carbon nanotube-reinforced composite plates resting on elastic foundations by dynamic relaxation method". Mechanics of Advanced Materials and Structures, Vol. 25, No 10, pp. 868-80, 2018.
[34] Golmakani ME, Kadkhodayan M. "An Investigation into the Thermoelastic Analysis of Circular and Annular Functionally Graded Material Plates". Mechanics of Advanced Materials and Structures, Vol. 21, No 1, pp. 1-13, 2014.
[35] Rezaiee-Pajand M, Vejdani Noghreiyan HR, Naghavi AR. "Four new methods for finding structural critical points". Mechanics Based Design of Structures and Machines, Vol. 41, No 4, pp. 399-420, 2013.
[36] Ni T, Zaccariotto M, Zhu Q-Z, Galvanetto U. "Coupling of FEM and ordinary state-based peridynamics for brittle failure analysis in 3D". Mechanics of Advanced Materials and Structures, Vol. 28, No 9, pp. 875-90, 2021.
[37] Papadrakakis M. "A method for the automatic evaluation of the dynamic relaxation parameters". Computer Methods in Applied Mechanics and Engineering, Vol. 25, No 1, pp. 35-48, 1981.
[38] Underwood P. "Dynamic relaxation (in structural transient analysis)". Computational Methods for Transient Analysis(A 84-29160 12-64) Amsterdam, North-Holland, Vol., No pp. 245-65, 1983.
[39] Qiang S. "An adaptive dynamic relaxation method for nonlinear problems". Comput Struct, Vol. 30, No 4, pp. 855-9, 1988.
[40] Zhang LG, Yu TX. "Modified adaptive dynamic relaxation method and its application to elastic-plastic bending and wrinkling of circular plates". Comput Struct, Vol. 33, No 2, pp. 609-14, 1989.
[41] Zhang LC, Kadkhodayan M, Mai YW. "Development of the maDR method". Comput Struct, Vol. 52, No 1, pp. 1-8, 1994.
[42] Topping BHV, Ivanyi P. Computer aided design of cable membrane structures. Scotland: Saxe-Coburg Publications; 2008. pp. 39-84.
[43] Barnes MR. "Form and stress engineering of tension structures". Structural Engineering Review, Vol. 6, No 3, pp. 175-202, 1994.
[44] Rajasekaran S. Numerical solution methods for natural frequencies and mode shapes in relation to structural dynamics during earthquakes. Structural dynamics of earthquake engineering: theory and application using mathematica and matlab: Elsevier Science; 2009.